Convenient Synthesis, Molecular Docking and *In-Vitro* Antibacterial Activity Studies of 3-*N*-Substituted 5-aryl(hetaryl)thieno[2,3-D]pyrimidin-4(3*H*)-Ones

Gagik Melikyan , Lusine Karapetyan * , Gayane Tokmajyan , Ravikumar Kapavarapu , Mane Tadevosyan , Hovik Panosyan , Anahit Hovhannisyan , Ashot Saghyan

Posted Date: 20 March 2026

doi: 10.20944/preprints202603.1622.v1

Keywords: 5-aryl(hetaryl)-3*N*-substituted-thieno[2,3-d]pyrimidin-4-ones; Gewald's reaction; 2-methyl¬aminomethyleneaminothiophenes; cyclocondensation; antibacterial activity

 doi:10.20944/preprints202603.1622.v1

Article

Convenient Synthesis, Molecular Docking and *In-Vitro* Antibacterial Activity Studies of 3-*N*-Substituted 5-aryl(hetaryl)thieno[2,3-D]pyrimidin-4(3*H*)-Ones

Gagik Melikyan [1], Lusine Karapetyan [2,3,*], Gayane Tokmajyan [3], Ravikumar Kapavarapu [4], Mane Tadevosyan [5], Hovik Panosyan [1,5], Anahit Hovhannisyan [1,6] and Ashot Saghyan [1,6]

[1] Institute of Pharmacy, Yerevan State University, Yerevan, 0025, Armenia
[2] Department of Organic Chemistry, Faculty of Chemistry, Yerevan State University, Yerevan, 0025 Armenia
[3] Chemical Research Center, Laboratory of Organic Chemistry, Yerevan 0025, Armenia
[4] Department of Biotechnology, University of Rzeszow, Pigonia 1, 35-310 Rzeszow, Poland
[5] Research Institute of Biology, Biology Faculty, Yerevan State University, Yerevan, 0025, Armenia
[6] Scientific and Production Center "Armbiotechnology" of NAS RA, Yerevan, 0056, Armenia
* Correspondence: lkarapetyan@ysu.am

Abstract

This study reports the convenient synthesis of a new series of sustainable heterocyclic compounds called 3-*N*-Substituted 5-aryl(hetaryl)-thieno[2,3-d]pyrimidin-4(3H)-ones, encompassing two biologically important pharmacophores namely thiophen and pyrimidine. A stepwise synthesis of 5-aryl(hetaryl)thieno[2,3-d]pyrimidine-4(3H)-ones with variable substituents at the N 3 position was proposed, which involves the synthesis of aromatic and heteroaromatic substituted 2-aminothiophenes, their condensation with N,N′-dimethylformamide dimethylacetal. Obtained 2-dimethylaminomethyleneamino-thiophenes condense with primary amines. This sequence of reactions leads to the production of new polyheteroconjugated systems with advantages like simple work up, easy separation of the products and chromatography-free purification. Structural elucidation was done by spectroscopic method and elemental analysis and have confirmed their molecular structure. The synthesized compounds were tested on their antibacteriial activity against Gram positive and Gram negative bacteria. Compound **6k** showed notable antibacterial activity compared to the standard drug (Gentamicin) against *S. aureus* bacteria. Compounds **6e** and **6k** were evaluated for their antimicrobial potential via molecular docking against *S. aureus* Aminoglycoside Phosphotransferase and *P. aeruginosa* TrmD. Compound **6k** exhibited superior binding affinity and an enhanced pharmacokinetic profile, positioning it as a promising lead for further optimization and development as an antimicrobial agent. However, as this study represents an initial screening, further in silico investigations are required for predicting antibacterial activity of target derivatives with calculated substituents. Overall, this work highlights the efficiency of a convenient approach for synthesizing 3-*N*-Substituted 5-aryl(hetaryl)-thieno[2,3-d]pyrimidin-4(3H)-ones and underscores their potential as promising scaffolds for the development of potent antibacterial agents.

Keywords: 5-aryl(hetaryl)-3*N*-substituted-thieno[2,3-d]pyrimidin-4-ones; Gewald's reaction; 2-methylaminomethyleneaminothiophenes; cyclocondensation; antibacterial activity

1. Introduction

Research in the field of synthesis of bioactive compounds is one of the promising areas in organic chemistry [1–4]. The increasing resistance of various pathogenic bacteria has become a major public health problem in recent years. The discovery of new, safe and highly effective bioactive compounds

 doi:10.20944/preprints202603.1622.v1

against pathogens is very urgent and still dominate in the synthesis of pharmaceutical compounds and drugs.

In this concept, the biological, bactericidal and medicinal activities of fused thiophenes have stimulated considerable research. Some aromatic derivatives of thienopyridines such as clopitogrel (Plovix), ticlopidine, tinoridine and prasugrel (Figure 1) have been used in medical practice for over 30 years as thrombolytic drugs for the prevention and treatment of myocardial infarction and diseases associated with atherosclerosis [5].

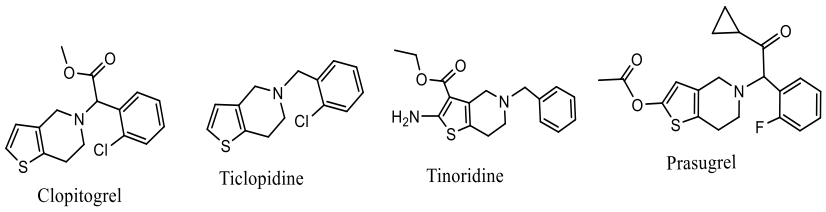

Figure 1. Aromatic derivatives of thienopyridines.

The derivatives of thieno[2,3-d]pyrimidin-4-ones possess a number of valuable biological properties and have a wide practical usage [6–8]. Several *N*-substituted-5-(2-furanyl)-thieno[2,3-d]pyrimidin-4(3*H*)-ones represent antimicrobial activity [9,10], the others, possessing aromatic and heterocyclic substituents are developing anti-inflammatory, antipyretic, anticonvulsant, ulcerogenic, antihypertensive and other activities [11–18]. Sufugolix, Relugolix, PRX-08066 and DDP-225 contain a thieno[2,3-d]pyrimidine ring and are approved for therapeutic use (Figure 2) [19]. The aromaticity of thieno[2,3-d]pyrimidine ring and ability to be easily functionalized make them excellent "privileged structures" for drug design, leading to better absorption, potency, and selectivity.

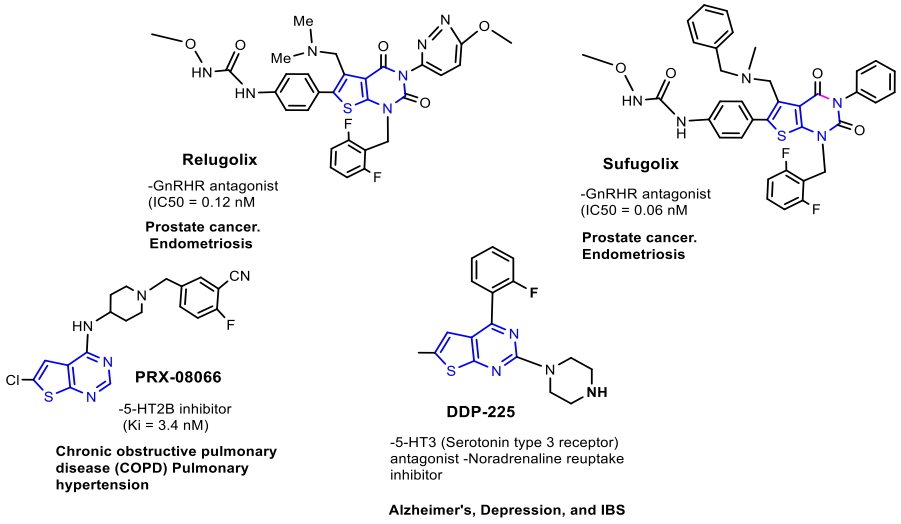

Figure 2. Structurs, biological targets and applications of some drug candidates containing the thieno[2,3-d]pyrimidine ring.(the thieno[2,3-d]pyrimidine scaffold is highlighted in blue).

On the basis of abovementioned statements our interest was focused on the synthesis of thieno[2,3-d]pyrimidin-4-ones with aromatic and heteroaromatic substituents at the position 5. It seems to be actual to propose a new approach for the synthesis of 5-aryl(hetaryl)thieno[2,3-d]pyrimidin-4-one derivatives with practically unlimited possibilities to introduce the desired substituent at the position 3.

Previously, we have developed a convenient and efficient method for the synhesis of 3-*N*-substituted thieno[2,3-d]pyrimidin-4-ones: construction of the pyrimidine ring by intramolecular cyclization of thiophene derivatives [20–23], which has general character. The proposed method allowed introducing the large variety of substituents, especially at the 3-*N* atom of the pyrimidinone

 doi:10.20944/preprints202603.1622.v1

ring, while the routine methods do not allow obtaining such derivatives in one step. Synthesis of new 3-*N*-substituted thieno[2,3-d] pyrimidin-4-ones has been of continuous interest in the synthesis of new functionalized thieno[2,3-d]pyrimidin-4-ones for their synthetic applications and biological evaluation [19–26].

Due to our interest in the development of new antibacterial compounds, the aim of the present work is to synthesize new 3-*N*-substituted 5-aryl(hetaryl)thieno[2,3-d]pyrimidin-4(3*H*)-ones derivatives and to evaluate the significance of this framework for antibacterial drug discovery. The acetyl derivatives of naphthalene, pyridine, thiophene were chosen for the synthesis of starting thiophenes.

2. Results and Discussion

Synthesis

The Gewald's reaction [27] for the synthesis of 2-aminothiophenes **3a-3c** was realized for aromatic and heteroaromatic derivatives of ylidenecyanoacetic acid ethyl esters **2a-2c**. The latest were synthesized by the interaction of acetyl derivatives of naphthalene, pyridine, thiophene **1a-1c** with ethyl cyanoacetate in the conditions of Cope method for Knoevenagel reaction. This sequence of reactions was a convenient approach to the synthesis of new polyheteroconjugated systems **3a-3c** (Scheme 1).

2-Amino-4-pyridin-4-yl-thiophene-3-carboxylic acid ethyl ester (**3b**) was also obtained by the three-component condensation (method B) of the 4-acetylpyridine **1b** with ethyl cyanoacetate and sulphur in the presence of diethyl amine in lower yields (26%). In the cases of 2-acetylnaphthalen **1a** and 2-acetylthiophene **1c** the three component reaction did not take place.

2-Aminothiophenes **3a-3c** smoothly reacted with *N,N'*-dimethylformamide dimethylacetal (DMF/DMA) in anhydrous xylene under reflux for 7 h with formation of the corresponding new β-dimethylaminomethyleneamino derivatives **4a-4c**, bearing easily leaving dimethylamino group, with yields up to 95%. It should be noted, that the same products were not obtained by refluxing the mixture of **3a-3c** with excess of DMFA in anhydrous ethanol in the presence of catalytic amounts of pyridine or sodium hydroxide

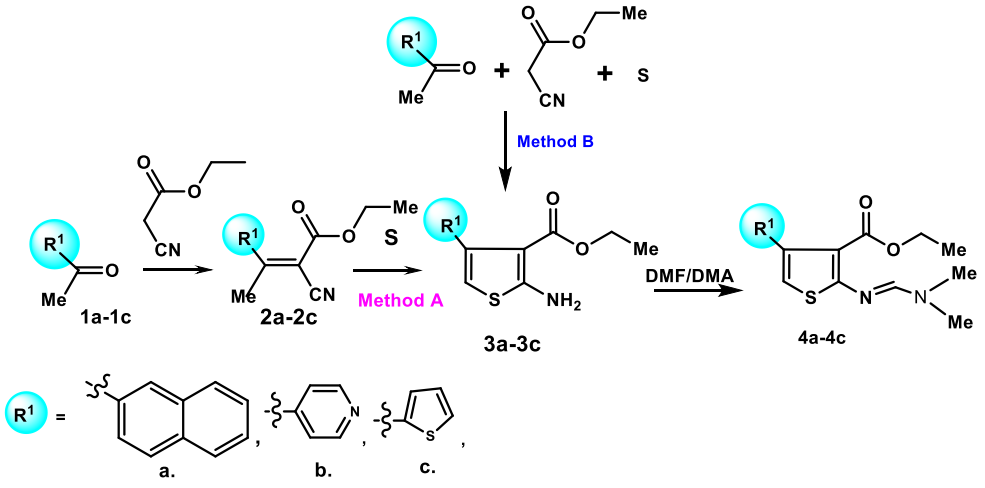

Scheme 1. Synthesis of 2-aminothiophenes **3a-3c** and 2-dimethylaminomethyleneaminothiophenes **4a-4c.**

The obtained products **4a-4c** lead to the novel derivatives of thieno[2,3-d]pyrimidin-4(3*H*)-ones **6a-6n** with modest to good yields by refluxing in anhydrous xylene with primary amines **5a-5l** (Scheme 2). These yields were obtained with the 1:3 molar ratio of the product **4a,b** to the primary amine **5a-5l**. Elimination of gaseous dimethylamine was used to monitor the progress of the reaction.

In the ^{1}H NMR spectra of the obtained compounds **6a–6n**, there are the signals of the =CH proton of the thiophen ring and N=CH proton of the pyrimidinone ring appear as singlets at 7.20- 7.48 and 8.02-8.60 ppm, respectively. In the ^{13}C NMR spectra of compounds **6a–6n**, there are signals of C2, C3,

 doi:10.20944/preprints202603.1622.v1

C4, C5 carbons of the thiophen ring (157.30-161.45, 128.14-135.07, 137.46-146.43, 126.11-127.74 ppm, respectively), N=CH carbon (146.40-148.34 ppm) and the carbonyl carbon (164.92-165.32 ppm) of the pyrimidinone ring. The elemental analyses of the synthesised compounds **4a-4c** and **6a–6n** were found within the limit of ± 0.4% of theoretical values.

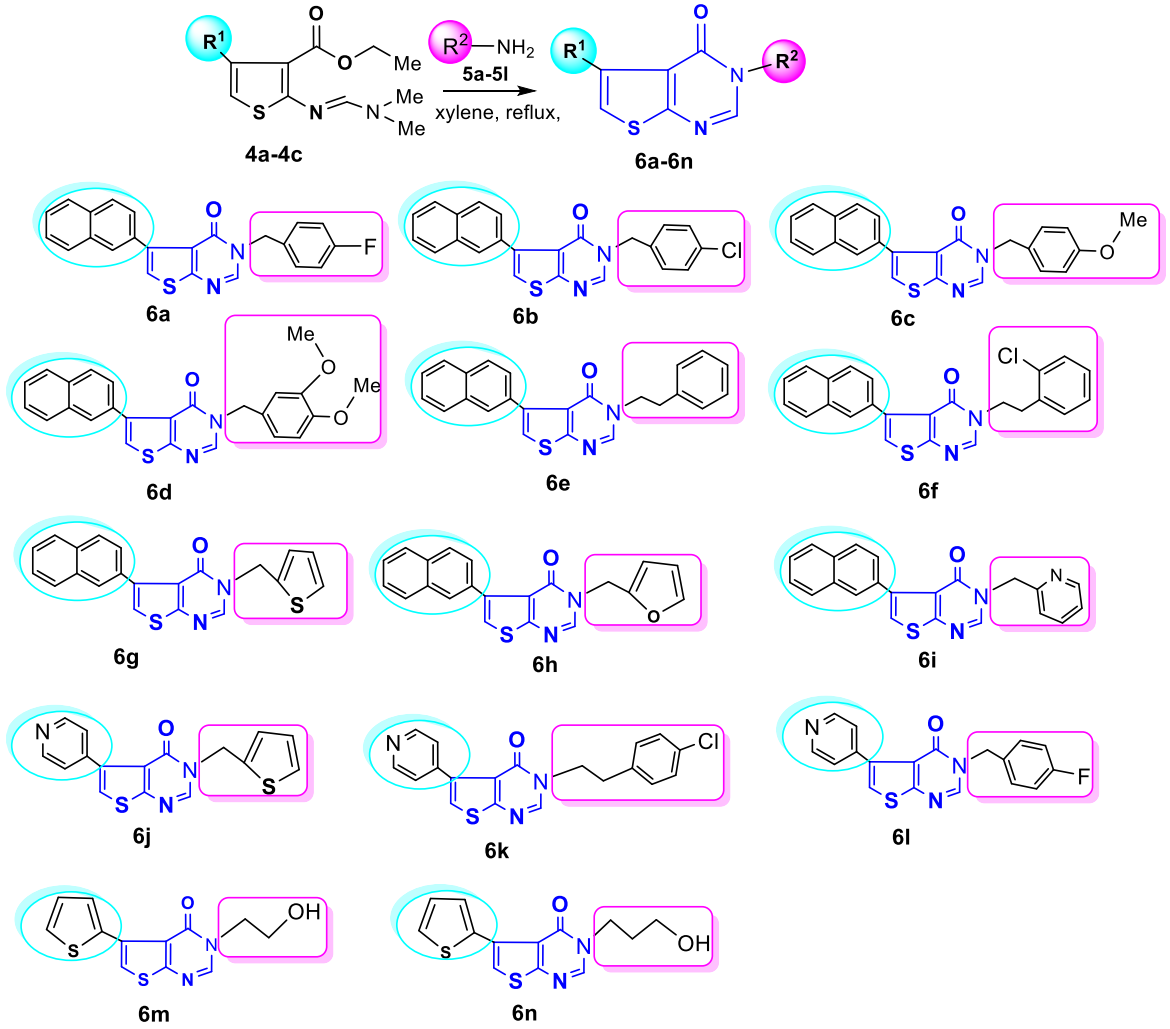

Scheme 2. Synthesis of 3-*N*-Substituted 5-aryl(hetaryl)thieno[2,3-d]pyrimidin-4(3*H*)-ones **6a-6n.**

Antibacterial Activity

All the new synthesized compounds **6a-6n** were evaluated for their antibacterial activities against two Gram-positive bacteria (*B. subtilis* WT-A1 and *S. aureus* MDC 5233) and three Gram-negative bacteria (*E. coli* VKPM-M17, *P. aeruginosa* GRP3, *S. typhimurium* MDC 1754). All strains were obtained from the microbial culture collection maintained by the Department of Biochemistry, Microbiology and Biotechnology at Yerevan State University (YSU).

Antibacterial activity was assessed using the agar well diffusion method. Bacterial cultures were first grown overnight in Müller-Hinton broth (MHB), then sub-cultured to fresh MHB and incubated at 37 °C until reaching an optical density of OD_{600} = 0.2. Subsequently, 100 µL of each bacterial suspension was evenly spread onto Müller-Hinton agar (MHA) plates.

The synthesized compounds **6a-6n** were dissolved in dimethyl sulfoxide (DMSO) to a final concentration of 2 mg/mL. For each test, 50 µL of the compound solution was added into wells punched into the agar using a sterile paper punch. Plates were then incubated at 37 °C for 24 hours. The diameters of the inhibition zones (IZ) around each well were measured in millimeters. Each test was performed in triplicate, and the mean value of the inhibition zones was recorded as an index of antibacterial activity. Gentamicin (10 µg/mL) served as the positive control, while 5% DMSO was used as the negative control (Table 1).

 doi:10.20944/preprints202603.1622.v1

Table 1. Antibacterial activity of the synthesized compounds **6a-6n**.

Compound	IZ diameters (mm) of tested compounds against reference bacterial strains				
	B. subtilis	*S. aureus*	*E. coli*	*P. aeruginosa*	*S. typhimurium*
6e	–	–	–	4	–
6k	–	10	–	–	–
Others	–	–	–	–	–

("–" indicates absence of an inhibition zone).

Among all the tested compounds **6k** demonstrated notable antibacterial activity, producing a 10 mm inhibition zone (IZ) against *S. aureus* in the well diffusion assay. Compound **6e** demonstrated low antibacterial activity, producing a 4 mm inhibition zone (IZ) against *P. aeruginosa* in the well diffusion assay. None of the compounds exhibited activity against the other tested strains at the specified concentration. These results indicate that specific structural features of the thieno[2,3-d]pyrimidin-4-one scaffold may be critical for antibacterial efficacy. Compound **6k**, in particular, appears to be a promising lead for further structural optimization and comprehensive biological evaluation.

3. Conclusions

A convenient stepwise synthesis of 3-*N*-Substituted 5-aryl(hetaryl)thieno[2,3-d]pyrimidin-4(3*H*)-ones **6a-6n** with variable substituents at the N(3) position is proposed. The reaction of acetyl derivatives of naphthalene, pyridine, thiophene **1a-1c** with ethyl cyanoacetate yielded ethyl esters of the corresponding ylidene cyanoacetic acids **2a-2c**. The latter reacted with sulfur to form substituted 2-aminothiophenes **3a-3c**, and their condensation with *N*,*N*′-dimethylformamide dimethylacetal afforded 2-dimethylaminomethyleneaminothiophenes **4a-4c,** which condensation with primary substituted amines **5a-5l** results in the construction of a pyrimidine ring. This reaction sequence leads to the production of new polyheteroderivative systems consisting of naphthalene, pyridine, thiophene, and pyrimidine rings. The synthesized compounds were structurally characterized and their antibacterial activity was in vitro evaluated against Gram-negative and Gram-positive bacteria. Compound **6e** demonstrated low antibacterial activity against *P. aeruginosa* bacteria. Compound **6k** demonstrated notable antibacterial activity against *S. aureus* bacteria. Molecular docking study demonstrated that **6k** achieves stronger, diversified interactions and superior binding affinity compared to **6e**, consistent with in vitro antibacterial trends. Conserved active-site recognition motifs with reference ligands elucidate the structural basis of activity. While ADMET profiling highlights of favorable pharmacokinetics of compound **6k**, its predicted mutagenicity warrants caution. These results position **6k** as a promising lead for antibacterial therapy with targeted safety optimization.

4. Materials and Methods

All chemicals were acquired from Sigma-Aldrich. They were used as received. The solvents were purified through standard procedures. ^{1}H and ^{13}C NMR spectra were recorded on Varian Mercury-300 MHz in DMSO-CCl_4 mixture (1:3) or on Bruker AVANCE 400 MHz spectrometer in $CDCl_3$. Chemical shifts (δ) in ppm are reported as quoted relative to the residual signals of $CHCl_3$-d (7.25 for ^{1}H NMR and 77.0 for ^{13}C NMR) or DMSO-d_6 (2.5 for ^{1}H NMR and 39.5 for ^{13}C NMR) as internal references. The coupling constants (J) are given in Hertz. Elemental analyses (C, H, and N) were performed using a Heraeus CHN–O–Rapid analyzer, and results agreed with calculated values. The purity of the isolated compounds and the reaction progress were monitored by TLC on "Silufol UV-254" plates using acetone–benzene (1 : 2) as eluent; spots were visualized by treatment with iodine vapor. The melting points were measured with an Electrothermal 9100 melting point apparatus.

Compounds **2a-2c** were prepared according to the method [28].

 doi:10.20944/preprints202603.1622.v1

Compounds **3a-3c** were prepared according to the Gewald's method [27].

General Procedure for the Syntheses of Compounds 2a-2c

A mixture of compounds **1a-1c** (500.0 mmol), ethyl cyanoacetate (500.0 mmol), β-alanine (5.0 mmol), glacial acetic acid (24mL) and benzene (100mL) was refluxed with Dean-Stark trap for 18 hours. The mixture was allowed to cool to ambient temperature, benzene (30mL) was added, and then the mixture was washed with water (3 x 30mL). The combined aqueous washings were shaken with benzene (15mL), then the combined benzene solutions were dried ($MgS0_4$) and the solvent was removed in vacuum. The residual oil was distilled under reduced pressure to give compounds **2a-2c,** which were used without further purification.

General Procedure for the Syntheses of Compounds 3a-3c

Method A. A mixture of compounds **2a-2c** (50.0 mmol), sulphur (50.0 mmol), diethylamine (5mmol) and absolute ethanol (25mL) was refluxed for 7 h. The mixture was allowed to cool to ambient temperature and the solvent was removed under reduced pressure to give compounds **3a-3c,** which were used without further purification.

Method B. A mixture of compounds **1b** (500.0 mmol), ethyl cyanoacetate (500.0 mmol), β-alanine (5.0 mmol), sulphur (500.0 mmol), diethylamine (50mmol) and absolute ethanol (50mL) was refluxed with Dean-Stark trap for 25 h. The mixture was allowed to cool to ambient temperature and the solvent was removed under reduced pressure to give compound **3b.**

General Procedure for the Syntheses of Compounds 4a-4c

A mixture of compounds **3a-3c** (10 mmol) and DMF/DMA (12 mmol) in an anhydrous xylene (12 mL) was refluxed for 3 h. The mixture was allowed to cool to ambient temperature, then light petroleum (5 mL) was added into the mixture. The precipitate was filtered, washed with ether, dried.

Ethyl 2-(((dimethylamino)methylene)amino)-4-(naphthalen-2-yl)thiophene-3-carboxylate (**4a**). Yellow solid; yield 95%, m. p. 104-105°C. Found, %: C 68.54; H 6.08; N 8.29; S 9.38. $C_{20}H_{20}N_2O_2S$ (352.45). Calculated, %: C 68.16; H 5.72; N 7.95; S 9.10. ^{1}H NMR (300 MHz, DMSO-d_6–CCl_4, 1:3) δ 1.10 (t, J = 7.1Hz, 3H, $OCH_2C\underline{H}_3$); 3.04 (br s, 3H, NCH_3); 3.12 (br s, 3H, NCH_3); 4.07 (q, J =7.1 Hz, 2H, $OC\underline{H}_2CH_3$); 6.62 (s, 1H, Th-H); 7.39- 7.48 (m, 3H, NAP-H); 7.74 (s, 1H, N=C$\underline{H}$); 7.78-8.01 (m, 4H, NAP-H).

Ethyl 2-(((dimethylamino)methylene)amino)-4-(pyridin-4-yl)thiophene-3-carboxylate (4b). Yellow solid; yield 87%, m. p. 97-98°C. Found, %: C 59.47, H 5.56, N 13.65, S 10.40. $C_{15}H_{17}N_3O_2S$ (303.39). Calculated, %: C 59.39, H 5.65, N 13.85, S 10.57. ^{1}H NMR (300 MHz, DMSO-d_6–CCl_4, 1:3) δ 1.10 (t, J =7.1 Hz, 3H, $OCH_2C\underline{H}_3$); 3.04 (br s, 3H, NCH_3); 3,12 (br s, 3H NCH_3); 4.07 (q, 2H, J = 7.1 Hz, $OC\underline{H}_2CH_3$); 6.69 (s,1H, Th-H); 7.19 (d, 2H, J = 5.0 Hz, Py-H-2,6); 7.74 (s, 1H, N=C$\underline{H}$); 8.46 (d, 2H, J = 5.0 Hz, Py-H-3,5).

Ethyl 5′-(((dimethylamino)methylene)amino)-[2,3′-bithiophene]-4′-carboxylate (4c). Yellow solid; yield 94.9%, m. p. 85-86°C. Found, %: C 54.27, H 5.35, N 9.00, S 20.91. $C_{14}H_{16}N_2O_2S_2$ (308.42). Calculated, %: C 54.52, H 5.23, N 9.08, S 20.79.^{1}H NMR (300 MHz, DMSO-d_6–CCl_4, 1:3) δ 1.20 (t, J =7.1, 3H,$OCH_2C\underline{H}_3$), 3.02 (br s, 3H, NCH_3), 3.10 (br s, 3H, NCH_3), 4.14 (q, 2H, J =7.1Hz, $OC\underline{H}_2CH_3$), 6.62 (s, 1H, Th-H), 6.97–7.00 (m, 2H, Th-H-2,4), 7.23 (dd, J_1 =4.7, J_2 =1.6, 1H, Th-H-3), 7.72 (s, 1H, N=C$\underline{H}$).

General Procedure for the Syntheses of Compounds 6a-6n

A mixture of dimethylaminomethyleneamino derivative **4a-4c** (10 mmol) and the corresponding primary amine **5a-5l** (35 mmol) in anhydrous xylene (7 mL) was refluxed for 30 h (extra 3 h after cessation of dimethyl amine isolation). The mixture was allowed to cool to ambient temperature, then light petroleum (8 mL) was added into the mixture. The precipitate was filtered, washed with ether and dried.

3-(4-Fluorobenzyl)-5-(naphthalen-2-yl)thieno[2,3-d]pyrimidin-4(3H)-one(6a). Beige powder, yield 67%, m. p. 166-167°C. Found, %: 71.81; H, 4.30; N, 7.62; S, 8.64. $C_{23}H_{15}FN_2OS$ (386.44). Calculated, %: C 71.49; H, 3.91; N, 7.25; S, 8.30. ^{1}H NMR (400 MHz, $CDCl_3$) δ 5.15 (s, 2H, CH_2); 6.98-7.05 (m, 2H, Ar-H-3,5), 7.26 (s, 1H, Th-H); 7.29-7.39 (m, 2H, Ar-H-2,6), 7.49-7.56 (m, 2H, NAP-H-3,4); 7.68-7.72 and 7.85-7.96 (m, 4H, NAP-H-5,6,7,8), 8.00 (s, 1H, NAP-H-1) 8.10 (s, 1H, N=C$\underline{H}$). ^{13}C NMR (125

 doi:10.20944/preprints202603.1622.v1

MHz, $CDCl_3$) δ 48.55 (CH_2), 115.90 (C(3)-Ar), 116.12 (C(5)-Ar), 121.46 (C(1)-NAP), 121.62 (C(6)-NAP), 127.08 (C(7)-NAP), 127.74 (C(5)-Th), 127.90 (C(3)-NAP), 128.07(C(4)-NAP), 128.22 (C(8)-NAP), 130.01 (C(5)-NAP), 130.09(C(6)-Ar), 131.66(C(2)-Ar), 131.70 (C(3)-Th), 132.96 (C(1)-Ar), 133.12 (C-NAP), 133.15 (C-NAP), 139.83 (C(2)-NAP), 146.43 (C(4)-Th), 157.31 (C=N) 161.45 (C(2)-Th), 163.91 (C(4)-Ar), 165.03 (C=O).

3-(4-Chlorobenzyl)-5-(naphthalen-2-yl)thieno[2,3-d]pyrimidin-4(3H)-one (6b). Beige powder, yield 59%, m. p. 144-146°C. Found, %: C, 68.92; H, 3.99; N, 7.32; S, 8.27. $C_{23}H_{15}ClN_2OS$ (402.90). Calculated, %: C, 68.57; H, 3.75; N, 6.95; S, 7.96. ^{1}H NMR (400 MHz, $CDCl_3$) δ 5.15 (s, 2H, CH_2); 7.26 (s, 1H, Th-H); 7.29-7.35 (m, 4H, Ar-H-2,3,5,6), 7.48-7.55 (m, 2H, NAP-H-3,4); 7.65-7.72 and 7.85-7.90 (m, 4H, NAP-H-5,6,7,8), 8.00 (s, 1H, NAP-H-1) 8.10 (s, 1H, N=C<u>H</u>). ^{13}C NMR (125 MHz, $CDCl_3$) δ 48.64 (CH_2), 121.49 (C(1)-NAP), 121.69 (C(6,7)-NAP), 126.20 (C(5)-Th), 126.23 (C(3)-NAP), 127.11 (C(4)-NAP), 127.89 (C(5)-NAP), C(8)-NAP), 128.09 (C(3,5)-Ar), 128.24 (C(2,6)-Ar), 129.27 (C(3)-Th), 129.53 (C(4)-Ar), 132.98 (C-NAP), 133.13 (C-NAP), 134.33 (C(2)-NAP), 134.43 (C(1)-Ar), 139.88 (C(4)-Th), 146.40 (C=N), 157.30 (C(2)-Th), 165.06 (C=O).

3-(4-Methoxybenzyl)-5-(naphthalen-2-yl)thieno[2,3-d]pyrimidin-4(3H)-one (6c). Beige powder, yield 68%, m. p. 130-131°C. Found, %: C, 72.72; H, 4.89; N, 7.39; S, 8.41. $C_{24}H_{18}N_2O_2S$ (398.48). Calculated, %: C, 72.34; H, 4.55; N, 7.03; S, 8.05. ^{1}H NMR (400 MHz, $CDCl_3$) δ 3.75 (s, 3H, OCH_3); 5.10 (s, 2H, CH_2); 6.85 (d, *J* = 7.9 Hz, 2H, Ar-H-3,5) 7.20 (s, 1H, Th-H); 7.28 (d, *J* = 7.9 Hz, 2H, Ar-H-2,6), 7.44-7.55 (m, 2H, NAP-H-3,4); 7.68-7.73 and 7.85-7.90 (m, 4H, NAP-H-5,6,7,8), 8.00 (s, 1H, NAP-H-1) 8.10 (s, 1H, N=C<u>H</u>). ^{13}C NMR (125 MHz, $CDCl_3$) δ 48.56 (CH_2), 55.25 (OCH_3), 114.34 (C(3,5)-Ar), 121.32 (C(1)-NAP), 126.04 (C(6)-NAP), 126.06 (C(7)-NAP), 126.94 (C(5)-Th), 127.64 (C(3)-NAP), 127.83 (C(4)-NAP), 127.90 (C(8)-NAP), 127.96 (C(5)-NAP), 128.14 (C(2,6)-Ar), 129.68 (C(3)-Th), 132.84 (C(1)-Ar), 133.03 (2C-NAP), 133.20 (C(2)-NAP), 139.69 (C(4)-Th), 146.52 (C=N), 157.29 (C(4)-Ar), 159.58 (C(2)-Th), 164.92 (C=O).

3-(3,4-Dimethoxybenzyl)-5-(naphthalen-2-yl)thieno[2,3-d]pyrimidin-4(3H)-one (6d). Beige powder, yield 65%, m. p. 154-155°C. Found, %: C 70.41; H 5.05; N 6.89; S 7.80. $C_{25}H_{20}N_2O_3S$ (428.05). Calculated, %: C 70.07; H 4.70; N 6.54; S 7.48. ^{1}H NMR (400 MHz, $CDCl_3$) δ 3.85 (s, 3H, $2OCH_3$); 5.10 (s, 2H, CH_2); 6.78-6.90 (m, 3H, Ar-H-2,5,6), 7.20 (s, 1H, Th-H); 7.48-7.52 (m, 2H, NAP-H-3,4); 7.68-7.70 and 7.85-7.90 (m, 4H, NAP-H-5,6,7,8), 8.00 (s, 1H, NAP-H-1) 8.10 (s, 1H, N=C<u>H</u>). ^{13}C NMR (125 MHz, $CDCl_3$) δ 48.93 (CH_2), 55.99 (OCH_3), 56.08 (OCH_3), 111.43 (C(2)-Ar), 111.69 (C(5)-Ar), 120.91(C(6)-Ar), 121.38 (C(1)-NAP), 121.46 (C(6)-NAP), 126.14 (C(7)-NAP), 126.16 (C(5)-Th), 127.02 (C(3)-NAP), 127.73 (C(4)-NAP), 127.94 (C(8)-NAP), 128.05 (C(5)-NAP), 128.20 (C(3)-Th), 128.32 (C-NAP), 132.92 (C-NAP), 133.10 (C(2)-NAP), 133.26 (C(1)-Ar), 139.77 (C(4)-Th), 146.53 (C=N), 149.26 (C(4)-Ar), 149.47(C(3)-Ar), 157.40 (C(2)-Th), 165.00 (C=O).

5-(Naphthalen-2-yl)-3-phenethylthieno[2,3-d]pyrimidin-4(3H)-one (6e). Beige powder, yield 77%, m. p. 118-119°C. Found, %: C 75.72; H 5.04; N, 7.69; S 8.71. $C_{24}H_{18}N_2OS$ (382.48). Calculated, %: C 75.37; H 4.74; N 7.32; S 8.38. ^{1}H NMR (400 MHz, $CDCl_3$) δ 3.05 (t, 2H, J = 7.2 Hz, $CH_2C\underline{H}_2Ph$); 4.18 (t, 2H, J = 7.2 Hz, $C\underline{H}_2CH_2Ph$); 7.10-7.18 (m, 2H, Ph), 7.25 (s, 1H, Th-H); 7.28-7.38 (m, 3H, Ph), 7.48-7.52 (m, 2H, NAP-H-3,4); 7.68-7.70 and 7.85-7.90 (m, 4H, NAP-H-5,6,7,8), 7.65 (s, 1H, NAP-H-1), 8.05 (s, 1H, N=C<u>H</u>). ^{13}C NMR (125 MHz, $CDCl_3$) δ 35.22 (CH_2), 48.61 (CH_2), 121.22 (C(1)-NAP), 126.08 (C(6)-NAP), 126.11 (C(7)-NAP), 126.99 (C(5)-Th), 127.01 (C(4)-NAP), 127.68 (C(3)-NAP), 127.90 (C(2,6)-Ar), 128.00 (C(8)-NAP), 128.18 (C(5)-NAP), 128.85 (C(3,5)-Ar), 128.91 (C(3)-Th), 132.89 (C-NAP), 133.07 (C-NAP), 133.17 (C(2)-NAP), 137.39 (C(1)-Ar), 139.58 (C(4)-Th), 146.60 (C=N), 157.28 (C(2)-Th), 165.16 (C=O).

3-(2-Chlorophenethyl)-5-(naphthalen-2-yl)thieno[2,3-d]pyrimidin-4(3H)-one (6f). Beige powder, yield 58%, m. p. 151-153°C. Found, %: C 69.49; H 4.40; Cl 8.87, N 7.02; S, 7.98. $C_{24}H_{17}ClN_2OS$ (416.92). Calculated, %: C 69.14; H 4.11; Cl 8.50, N 6.72; S, 7.69. ^{1}H NMR (400 MHz, $CDCl_3$) δ 3.22 (t, J =7.2 Hz, 2H, $CH_2C\underline{H}_2C_6H_4$); 4.25 (t, J =7.2 Hz, 2H, $C\underline{H}_2CH_2C_6H_4$), 7.1- 7.28 and 7.35-7.45 (m, 4H, Ar-H-3,4,5,6), 7.26 (s, 1H, Th-H); 7.48-7.55 (m, 2H, NAP-H-3,4); 7.65 (s, 1H, NAP-H-1), 7.62-7.72 and 7.85-7.96 (m, 4H, NAP-H-5,6,7,8), 8.02 (s, 1H, N=C<u>H</u>). ^{13}C NMR (125 MHz, $CDCl_3$) δ 33.12 (CH_2), 46.56 (CH_2), 121.26 (C(1)-NAP), 121.33 (C(6)-NAP), 126.15 (C(7)-NAP), 126.17

 doi:10.20944/preprints202603.1622.v1

(C(6)-Ar), 127.07 (C(5)-Ar), 127.37 (C(4)-Ar), 127.74 (C(5)-Th), 127.93 (C(4)-NAP), 128.03 (C(3)-NAP), 128.24 (C(8)-NAP), 128.78 (C(5)-NAP), 129.86 (C(3)-Ar), 131.48 (C(3)-Th), 132.97 (C(2)-Ar), 133.15 (C-NAP), 133.21 (C-NAP), 134.15 (C(2)-NAP), 135.07 (C(4)-Th), 139.65 (C(1)-Ar), 146.59 (C=N), 157.44 (C(2)-Th), 165.23 (C=O).

5-(Naphthalen-2-yl)-3-(thiophen-2-ylmethyl)thieno[2,3-d]pyrimidin-4(3H)-one (6g). Beige powder, yield 58%, m. p. 147-148°C. Found, %: C 67.36; H 3.77; N7.48; S 17.12. $C_{21}H_{14}N_2OS_2$ (374.48). Calculated, %: C 67.36; H 3.77; N7.48; S 17.12. . ^{1}H NMR (400 MHz, $CDCl_3$) δ 5.3 (s, 2H, CH_2); 6.92 and 6.96 (dd, 1H, J_1=5.1, J_2=3.5Hz), 7.10 and 7.12 (dd, 1H, J_1=3.5, J_2=1.2Hz), 7.22 (s, 1H, Th-H); 7.27(dd, J_1=5.1, J_2=1.2Hz), 7.48-7.58 (m, 2H, NAP-H-3,4); 7.62-7.72 and 7.85-7.96 (m, 4H, NAP-H-5,6,7,8), 8.01 (s, 1H, NAP-H-1), 8.12 (s, 1H, N=CH). ^{13}C NMR (125 MHz, $CDCl_3$) δ 43.72 (CH_2), 121.22 (C(5)-Th(2)), 121.47 (C(1)-NAP), 126.05 (C(6)-NAP), 126.08 (C(7)-NAP), 126.64 (C(3)-Th(2)), 126.99 (C(4)-Th(2)), 127.09 (C(5)-Th(1)), 127.64 (C(4)-NAP), 127.84 (C(3)-NAP), 127.96 (C(8)-NAP), 127.98 (C(5)-NAP), 128.14 (C(3)-Th), 132.85 (C-NAP), 133.02 (C-NAP), 133.07 (C(2)-NAP), 137.46 (C(4)-Th(1)), 139.69 (C(2)-Th(2)), 146.08 (C=N), 156.90 (C(2)-Th(1)), 164.94 (C=O).

3-(Furan-2-ylmethyl)-5-(naphthalen-2-yl)thieno[2,3-d]pyrimidin-4(3H)-one (6h). Beige powder, yield 44%, m. p. 120-121°C. Found, %: C 70.71; H 4.29; N 8.15; S 9.31. $C_{21}H_{14}N_2O_2S$ (358.42). Calculated, %: C 70.37; H 3.94; N 7.82; S 8.94. ^{1}H NMR (400 MHz, $CDCl_3$) δ 5.15 (s, 2H, CH_2); 6.31 and 6.32 (dd, 1H, J_1=5.1, J_2=3.5Hz, Fur-H-3), 6.44 and 6.46 (dd, 1H, J_1=3.5, J_2=1.2Hz, Fur-H-4), 7.22 (s, 1H, Th-H); 7.72 and 7.74 (dd, J_1=5.1, J_2=1.2Hz, Fur-H-5), 7.48-7.58 (m, 2H, NAP-H-3,4); 7.85-7.95 (m, 4H, NAP-H-5,6,7,8), 7.98 (s, 1H, NAP-H-1), 8.18 (s, 1H, N=CH). ^{13}C NMR (125 MHz, $CDCl_3$) δ 41.61 (CH_2), 110.27 (C(3)-Fur), 110.27 (C(4)-Fur), 121.34 (C(1)-NAP), 121.42 (C(6)-NAP), 126.11 (C(7)-NAP), 127.14 (C(5)-Th), 127.03 (C(4)-NAP), 127.70 (C(3)-NAP), 127.89 (C(8)-NAP), 128.03 (C(5)-NAP), 128.20 (C(3)-Th), 132.92 (C-NAP), 133.09 (C-NAP), 133.16 (C(2)-NAP), 139.76 (C(4)-Th), 143.23 (C(5)-Fur), 146.3 (C(2)-Fur), 148.34 (C=N), 156.92 (C(2)-Th), 165.00 (C=O).

5-(Naphthalen-2-yl)-3-(pyridin-2-ylmethyl)thieno[2,3-d]pyrimidin-4(3H)-one (6i). Beige powder, yield 44%, m. p. 120-121°C. Found, %: C 71.91; H 4.42; N 11.71; S 9.01. $C_{22}H_{15}N_3OS$ (369.44). Calculated, %: C 71.52; H 4.09; N 11.37; S 8.68. ^{1}H NMR (400 MHz, $CDCl_3$) δ 5.24 (s, 2H, CH_2); 7.16, 7.18 and 7.20 (ddd, 1H, *J*=7.5; 4.8; 1.0 Hz, Py-H-), 7.22 (s, 1H, Th-H); 7.36 and 7.38 (dd, J_1=5.1, J_2=1.2Hz, Py-H-5), 7.48-7.58 (m, 2H, NAP-H-3,4); 7.60, 7.62 and 7.64 (ddd, 1H, *J*=7.5; 4.8; 1.0 Hz, Py-H-4), 7.66 and 7.68 (dd, 1H, 1H, J_1=5.1, J_2=3.5Hz, Py-H-5), 7.83-7.91 (m, 3H, NAP-H-5,6,7,8), 7.98 (s, 1H, NAP-H-1), 8.38 (s, 1H, N=CH). 8.51 and 8.53 (dd, 1H, J_1=5.1, J_2=3.5Hz, Py-H-6). ^{13}C NMR (125 MHz, $CDCl_3$) δ 50.60 (CH_2), 121.29 (C(5)-Py), 121.33 (C(3)-Py), 123.14 (C(6)-NAP), 123.20 (C(7)-NAP), 126.09 (C(1)-NAP), 126.11 (C(5)-Th), 127.02 (C(4)-NAP), 127.70 (C(3)-NAP), 127.91 (C(8)-NAP), 127.98 (C(5)-NAP), 128.20 (C(3)-Th), 132.91 (C-NAP), 133.10 (C-NAP), 133.24 (C(2)-NAP), 137.02 (C(4)-Py), 139.73 (C(4)-Th), 147.46 (C=N), 149.71 (C(6)-Py), 154.78 (C(2)-Py), 157.28 (C(2)-Th), 165.32 (C=O).

5-(Pyridin-4-yl)-3-(thiophen-2-ylmethyl)thieno[2,3-d]pyrimidin-4(3H)-one (6j). Beige crystals, yield 81.5%, m. p. 228-229°C. Found, %: C 58.84, H 3.63, N 12.78, S 19.55. $C_{16}H_{11}N_3OS_2$ (325.40). Calculated, %: C 59.06, H 3.41, N 12.91, S 19.71. ^{1}H NMR (300 MHz, DMSO) δ 5.38 (s, 2H, CH_2), 6.92 (dd, 1H, J_1=5.1, J_2=3.5Hz), 7.22 (dd, 1H, J_1=3.5, J_2=1.2Hz), 7.25-7.28 (m, 2H), 7.47 (s, 1H, Th-H), 7.48-7.50 (m, 2H), 8.53-8.56 (m, 2H), 8.57 (s, 1H, N=CH).

3-(4-Chlorophenyl)-ethyl-5-pyridin-4-yl)thieno[2,3-d]pyrimidin-4(3H)-one (6k). Beige crystals, yield 41.36%, m. p.173-174°C. Found, %: C 61.81, H 3.80, Cl 9.48, N 11.27, S 8.61. $C_{19}H_{14}ClN_3OS$ (367.86). Calculated, %: C 62.04, H 3.84, Cl 9.64, N 11.42, S 8.72. ^{1}H NMR (300 MHz, DMSO) δ 3.01 (t, 2H, J_2 = 3.5Hz, CH_2), 4.00 (t, 2H, J_2 = 3.5Hz, CH_2), 7.24 – 7.27 (m, 4H, C_6H_4), 7.44 (d, 2H, J= 3.5Hz, Py-H), 7.48 (s, 1H, Th-H), 8.24 (s, 1H, N=CH), 8.56 (d, 2H, J=3.5Hz, Py-H).

3-(4-Fluorobenzyl)-5-(pyridin-4-yl)thieno[2,3-d]pyrimidin-4(3H)-one (6l). Beige crystals, yield 87.0%, m. p. 177-178°C. Found, %: C 63.80, H 3.51, F 5.56, N 12.32, S 9.38. $C_{18}H_{12}FN_3OS$ (337.37). Calculated, %: C 64.08, H 3.59, F 5.63, N 12.45, S 9.50. ^{1}H NMR (300 MHz, DMSO) δ 5.18 (s, 2H, CH_2), 6.97–7.06 (m, 2H, C_6H_4), 7.43-7.52 (m, 2H, C_6H_4), 7.47 (s, 1H, Th-H), 7.52 (d, 2H, J=3.5Hz, Py-H), 8.53 (d, 2H, J=3.5Hz, Py-H), 8.60 (s, 1H, N=CH).

 doi:10.20944/preprints202603.1622.v1

3-(2-Hydroxyethyl)-5-(thiophen-2-yl)thieno[2,3-d]pyrimidin-4(3H)-one (6m): Beige crystals, yield 39.9%, m. p. 134-135°C. Found, %: C 51.99, H 3.53, N 9.97, S 22.79. $C_{12}H_{10}N_2O_2S_2$ (278.34). Calculated, %: C 51.78, H 3.62, N 10.06, S 23.04. ^{1}H NMR (300 MHz, DMSO) 3.69 (gt, 2H, J_1 = 5.3, J_2=5.1Hz, $CH_2C\underline{H}_2OH$); 4.06 (t, 2H, J=5.1Hz, $C\underline{H}_2CH_2OH$); 4.70 (t, 1H, J=5.3Hz, OH); 7.03 (dd, 1H, J_1 = 5.1, J_2=3.6Hz, Th(2)-H-4); 7.31 (dd, 1H, J_1=5.1, J_2=1.0Hz, Th(2)-H-3); 7.34 (s, 1H, Th(1)-H); 7.60 (dd, 1H, J_1=3.6, J_2=1.0Hz, Th(2)-H-5); 8.20 (s, 1H, N=C$\underline{H}$).

3-(3-Hydroxypropyl)-5-(thiophen-2-yl)thieno[2,3-d]pyrimidin-4(3H)-one (6n): Beige crystals, yield 34.7%, m. p. 115-116°C. Found, %: C 53.28, H 4.01, N 9.51, S 21.73. $C_{13}H_{12}N_2O_2S_2$ (292.37). Calculated, %: C 53.40, H 4.14, N 9.58, S 21.93. ^{1}H NMR (300 MHz, DMSO) 1.89 (tt, 2H, J_1=6.8, J_2=5.7Hz, $CH_2C\underline{H}_2CH_2OH$); 3.49 (t, 2H, J=5.7 Hz, $CH_2CH_2C\underline{H}_2OH$); 4.10 (t, 2H, J=6.8 Hz, $C\underline{H}_2CH_2CH_2OH$); 4.36 (br s, 1H, OH), 7.03 (dd, 1H, J_1=5.1, J_2=3.6Hz,); 7.30 (dd, 1H, J_1=5.1, J_2=1.0Hz); 7.34 (s, 1H, Th(1)-H); 7.59 (dd, 1H, J_1=3.6, J_2=1.0Hz); 8.30 (s, 1H, N=C$\underline{H}$).

Molecular Docking Studies

To investigate the structural basis of the antimicrobial activity of thieno-pyrimidone derivatives 6e and 6k, molecular docking studies were carried out using AutoDock Vina within the PyRx 0.8 virtual screening environment [29]. The molecular determinants underlying the antidiabetic potential of the synthesized compounds were investigated through computational docking studies performed against Staphylococcus aureus Aminoglycoside Phosphotransferase (APH(2″)-Ia, co-crystallized with Gentamicin C1 (51G) (PDB ID: 5IQC, 2.30 Å resolution) [30] and Pseudomonas aeruginosa tRNA (Guanine37-N1)-Methyltransferase (TrmD) protein targets.The TrmD (PDB ID: 5ZHM, 2.65 Å resolution) is co-crystallized with a thienopyrimidinone derivative (9D3) [31] were utilized for the docking simulations.

Aminoglycoside Phosphotransferase and TrmD were chosen as relevant targets to rationalize and validate the in vitro antimicrobial activity of the tested compounds. The binding affinities and interaction patterns of the compounds were analyzed and compared with those of the co-crystallized reference inhibitors, Gentamicin and 9D3, to gain insights into potential inhibitory mechanisms. These targets were specifically selected because the compounds demonstrated notable antibacterial activity, particularly against Staphylococcus aureus and *P. aeruginosa* strains. In line with the *in vitro* assays using Gentamicin as a comparator, *S. aureus* Aminoglycoside Phosphotransferase co-crystallized with Gentamicin was included for docking studies. Similarly, TrmD from *P. aeruginosa* co-crystallized with 9D3, structurally similar to the tested compounds due to its thienopyrimidone scaffold was selected to explore structure-based interactions potentially underlying the observed antibacterial effects.

Protein structures were preprocessed for molecular docking using the Dock Prep tool in UCSF Chimera. The preparation steps involved removal of co-crystallized ligands and water molecules, reconstruction of missing atoms or residues, and energy minimization to optimize geometry. Polar hydrogens were added, and Gasteiger charges were assigned to accurately represent electrostatics. The finalized protein models were then saved in PDBQT format for subsequent docking simulations.

Ligand structures were initially sketched in 2D using ChemDraw and subsequently converted into 3D geometries for further refinement. Energy minimization was carried out using the MMFF94 force field with the conjugate gradient algorithm in PyRx's Open Babel module, producing stable low-energy conformations. The optimized ligands were then exported in PDBQT format for docking studies with AutoDock.

Docking simulations in AutoDock Vina were performed by defining a focused grid around the active sites of the target proteins. For *S. aureus* Aminoglycoside Phosphotransferase, the grid center was set at X: 34.328, Y: -0.559, Z: 64.661, while for *P. Aeruginosa* TrmD, it was positioned at X: 45.373, Y: 113.745, Z: 16.516. A cubic grid box measuring 25 Å on each side with a spacing of 0.375 Å was employed to allow accurate sampling of ligand orientations within the binding pocket.

Following docking, the ligand–receptor complexes were examined to characterize binding modes and interaction patterns using ChimeraX [32] and BIOVIA Discovery Studio 2021.

 doi:10.20944/preprints202603.1622.v1

Molecular docking was carried out using the software's default parameters, producing ten binding conformations per compound. The conformation exhibiting the lowest predicted binding energy was chosen for detailed analysis of ligand–receptor interactions.

The docking protocol was validated by re-docking 9D3 into its native co-crystallized binding site. The superimposition of the re-docked ligand onto the original crystal structure yielded an RMSD of 0.93 Å, demonstrating that the docking setup reliably reproduces the experimentally observed binding conformation.

Figure 3. Binding affinity plot of **6e** and **6k** compounds with *S.aureus* Aminoglycoside Phosphotransferase and *P.aeruginosa* TrmD.

Molecular interaction profile with *S. aureus* Aminoglycoside Phosphotransferase

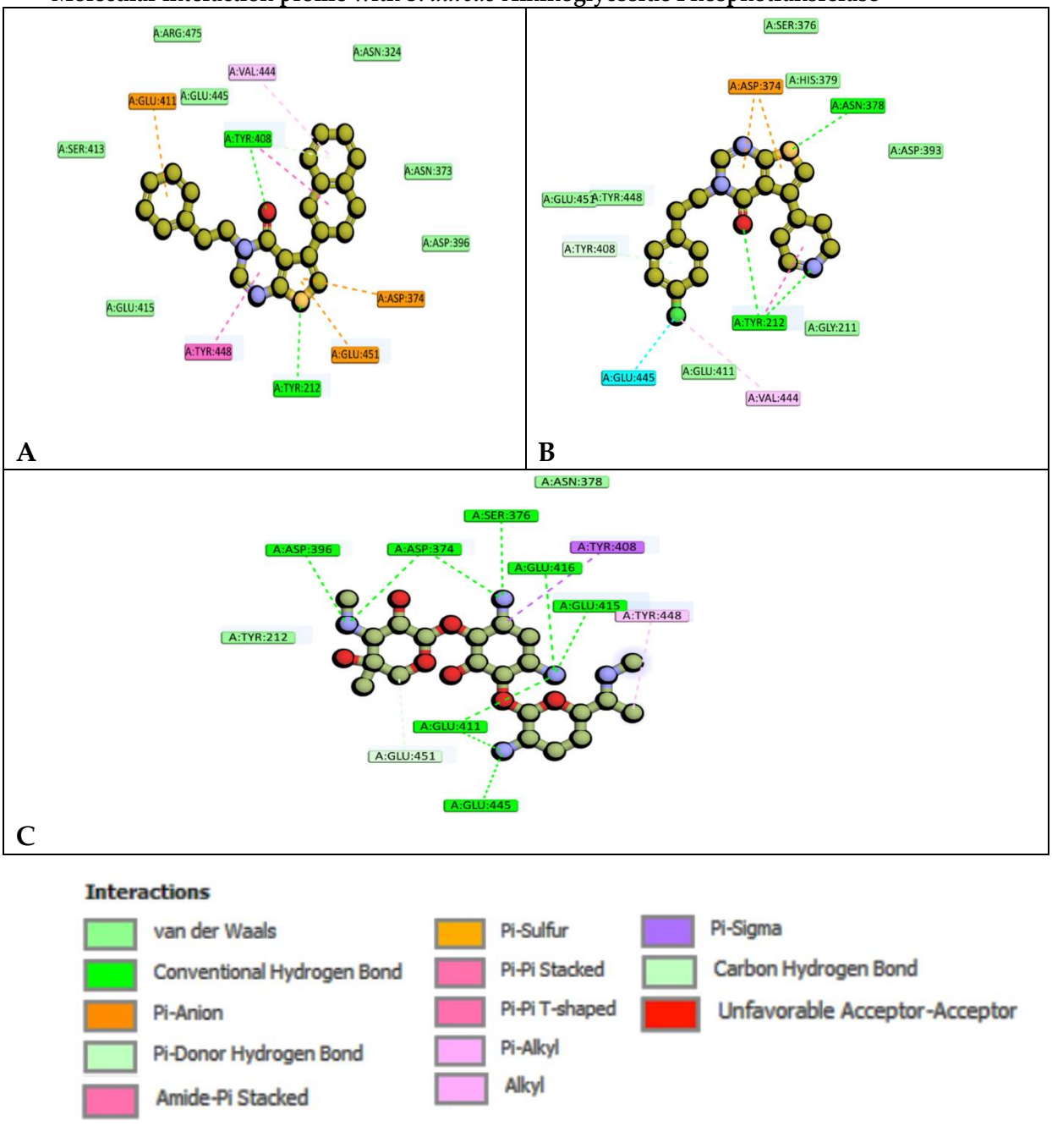

Figure 4. 2D molecular representation of interactions of compounds A)**6e**, B)**6k**, and C) Gentamicin with the active site residues of the *S. aureus* Aminoglycoside Phosphotransferase protein. Interactions were displayed as color coded dashed lines, green lines indicated the H–bonds.

 doi:10.20944/preprints202603.1622.v1

Table 2. Binding energy and interaction summary with *S. aureus* Aminoglycoside Phosphotransferase.

Compounds	Binding Energy (K.cal/mol)	Interacting Amino acids	Nature of interactions
6e	-7.3	**TYR408**, **TYR212**, GLU411, TYR448, VAL444, ASP374, GLU451, GLU415, SER413, GLU445, ARG475, ASN324, ASN373, ASP396	H-bond, π-sulfur, π-π stacked, π-π T shaped, π-alkyl, π-anion, π-donor hydrogen bond, van der waals
6k	-7.8	**ASN378, TYR212**, ASP374, GLU445, VAL444, TYR408, GLU451, TYR448, SER376, HIS379, ASP393, GLY211, GLU411	H-bond, π-anion, π-π stacked, π-π T shaped, halogen, alkyl, π-anion, π-donor hydrogen bond, van der waals
Gentamicin	-8.2	**ASP396, ASP374, SER376, GLU416, GLU415, GLU411, GLU445,** TYR408, TYR448, GLU451, TYR212, ASN378	H-bond, π-sigma, π-alkyl, C-H bond, van der waals

H-bond forming residues are bolded.

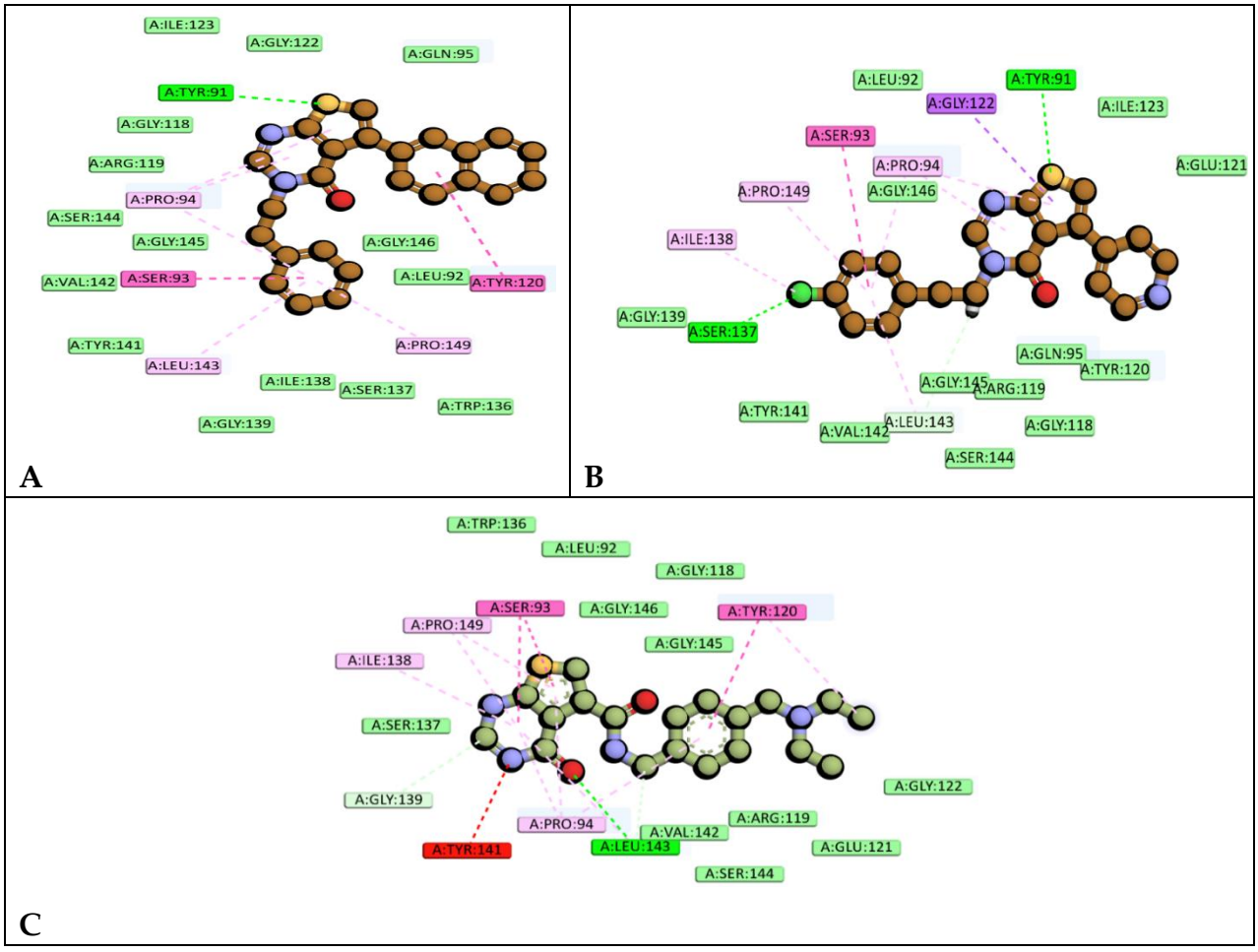

 doi:10.20944/preprints202603.1622.v1

Figure 5. 2D molecular representation of interactions of compounds A)**6e**, and B)**6k**, and C)9D3 with the active site residues of the *P. aeruginosa* TrmD protein. Interactions were displayed as color coded dashed lines, green lines indicated the H–bonds.

Table 3. Binding energy and interaction summary with *P. aeruginosa* TrmD.

Compounds	Binding Energy (K.cal/mol)	Interacting Amino acids	Nature of interactions
6e	-7.1	**TYR91,** TYR120, SER93, PRO94, LEU143, PRO149, ILE123, GLY122, GLN95, GLY118, ARG119, SER144, GLY145, VAL142, GLY146, LEU92, TYR141, ILE138, SER137, TRP136, GLY139	H-bond, π-sulfur, π-π T shaped, Amide-π stacked, π-alkyl, van der waals
6k	-7.5	**TYR91, SER137,** SER93, GLY122, PRO94, PRO149, ILE138, LEU143, GLY139, TYR141, VAL142, SER144, GLY118, ARG119, GLY145, GLN95, TYR120, GLU121, ILE123, GLY146, LEU92	H-bond, π-sigma, π-sulfur, π-alkyl, alkyl, Amide-π stacked, C-H bond, van der waals
9D3	-6.8	**LEU143**, TYR120, SER93, PRO149, ILE138, GLY139, PRO94, SER137, TRP136, LEU92, GLY146, GLY145, GLY118, GLY122, ARG119, GLU121, SER144, VAL142, TYR141	H-bond, π-π T shaped, Amide-π stacked, π-alkyl, C-H bond, van der waals, unfavourable acceptor-acceptor interactions

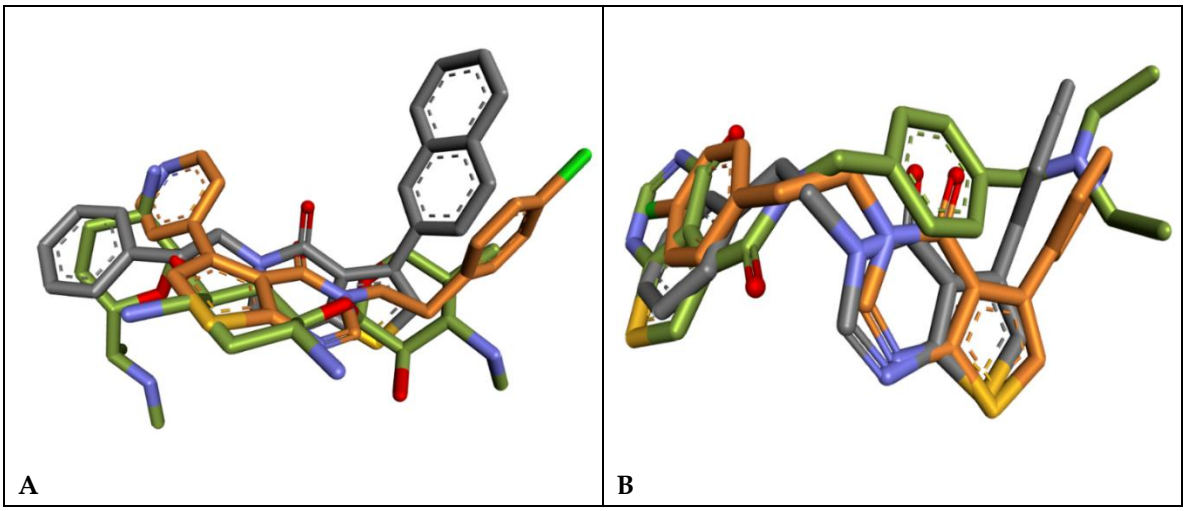

Figure 6. Molecular aligment of the binding poses of compounds **6e** (grey), **6k** (orange) and Gentamicin(A) and 9D3 (B) in gold color in the actives of the *S. aureus* Aminoglycoside 9(A) and *P. aeruginosa* TrmD (B) proteins for comparative three dimentional steric space visulazation with the reference compounds.

 doi:10.20944/preprints202603.1622.v1

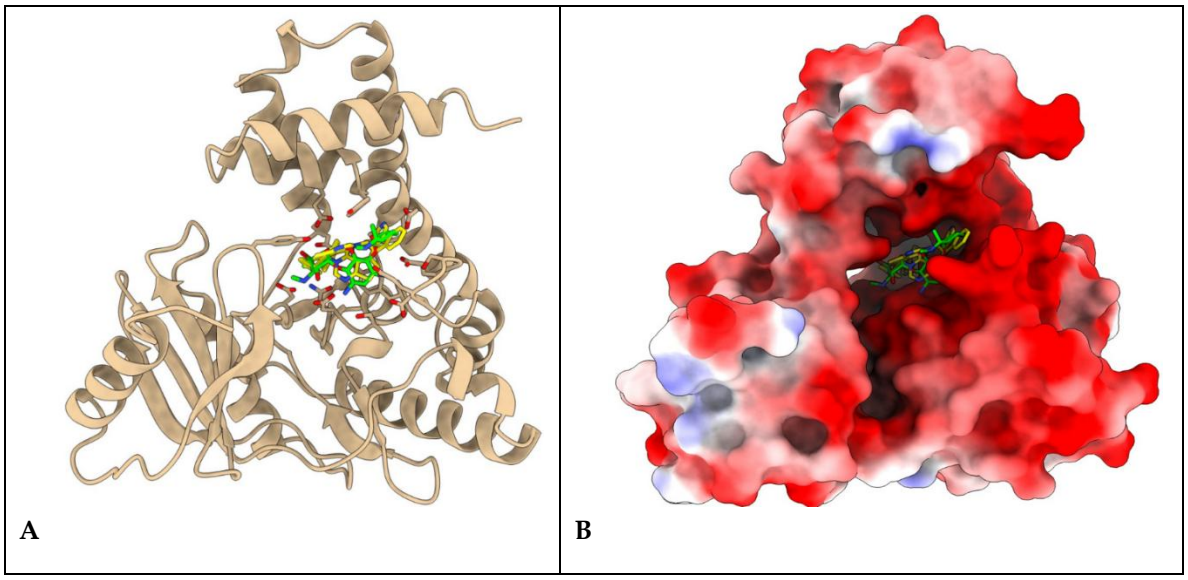

Figure 7. Protein ligand complexes representing the A) binding site of **6e** and **6k** (yellow) with Gentamicin (green) in stick model and B) their respective orientations and topology of the active site pocket of *S. aureus* Aminoglycoside Phosphotransferase.

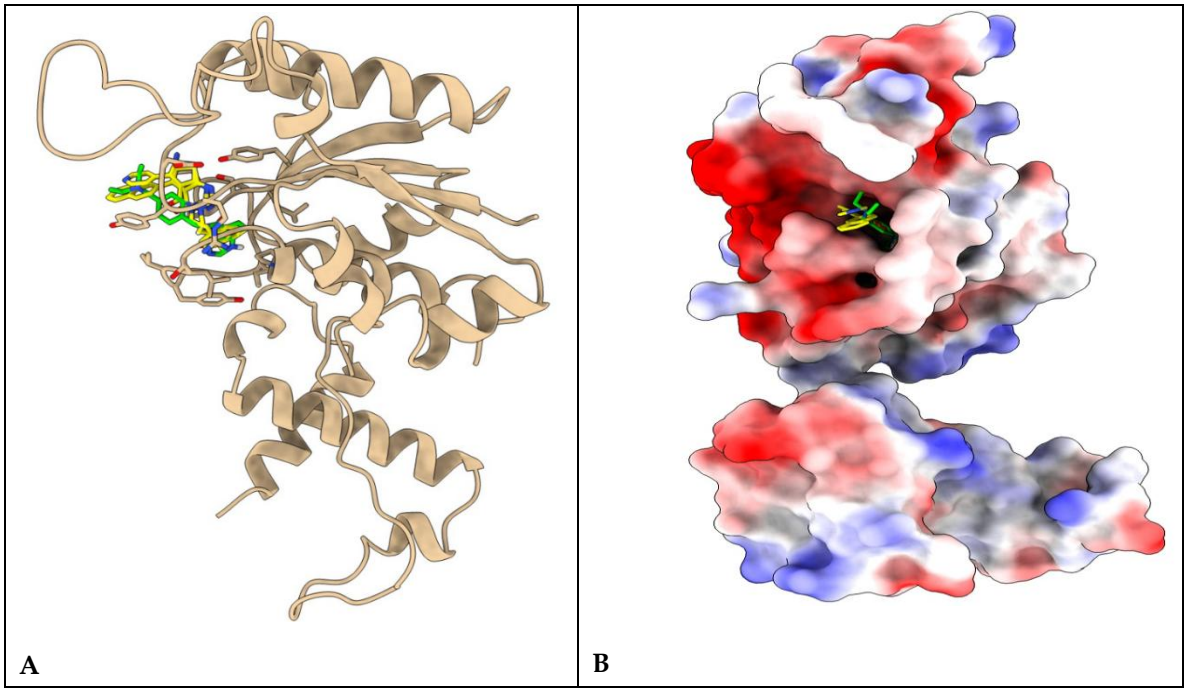

Figure 8. Protein ligand complexes representing the A) binding site of **6e** and **6k** (yellow) with 9D3 (green) in stick model and B) their respective orientations and topology of the active site pocket of *P. aeruginosa* TrmD.

Molecular interaction profile of compounds with Aminoglycoside Phosphotransferase

Docking-based binding affinity results against *S. aureus* Aminoglycoside phosphotransferase showed that compound **6k** (–7.8 kcal/mol) binds more strongly than compound **6e** (–7.3 kcal/mol) and displays a binding affinity close to that of gentamicin (–8.2 kcal/mol). These results correspond well with the relative *in-vitro* antibacterial activities of the compounds (Table 2).

Gentamicin C1 comprises of three structural moieties; garosamine, 2-deoxystreptamine, and purpurosamine rich in hydroxyl and amine functionalities. These functional groups enable an extensive hydrogen-bonding network with key residues, particularly involving the $–NH_2$ groups, which form multiple hydrogen bonds with ASP396, ASP374, SER376, GLU416, GLU415, GLU411, and GLU445. In addition, TYR408 engages in a $\pi–\sigma$ interaction with the 2-deoxystreptamine ring.

 doi:10.20944/preprints202603.1622.v1

The methylamine substituent exhibits a π–alkyl interaction with TYR448, while GLU451 contributes a C–H bond interaction with the garosamine ring, collectively stabilizing the ligand within the binding pocket.

Compound **6e**, bearing naphthyl and phenethyl substituents on the thienopyrimidinone scaffold, exhibits two key hydrogen-bond interactions with the active-site residues TYR212 and TYR408. The residues GLU411, GLU451, and ASP374 participate in π–anion interactions with the phenyl and thieno rings. Furthermore, VAL444 and TYR408 engage in π–alkyl, π–π T-shaped, and π-donor hydrogen-bond interactions with the naphthyl moiety, while TYR448 forms a π–π stacking interaction with the pyrimidinone core. Collectively, these interactions indicate that both the substituent aromatic rings and the heterocyclic backbone contribute to a diverse and complementary interaction profile that stabilizes compound 6e within the active site. In addition, nearby residues SER413, GLU415, ARG475, GLU445, ASN324, ASN373, and ASP396 contribute van der Waals interactions, contributing to the further reinforced ligand binding.

Compound **6k**, featuring pyridyl and 4-chlorphenethyl substituents on the core scaffold, exhibited a well-defined interaction profile within the active site. A hydrogen-bond interaction was observed between the sulfur atom of the thieno ring and ASN378, while the pyridine nitrogen and 4-oxo group of the pyrimidone ring formed hydrogen bonds with TYR212. In addition, ASP374 engaged in a π–anion interaction with the thieno-pyrimidone scaffold. The TYR212 residue further contributed a π–π stacking interaction with the pyridyl ring, whereas TYR408 participated in a π-donor hydrogen-bond interaction with the chloro-substituted phenyl ring. The chloro substituent established halogen bonding interactions with GLU445 and alkyl contacts with VAL444. Additionally, surrounding residues including GLU411, TYR448, GLU451, SER376, HIS379, GLY211, and ASP393 formed stabilizing van der Waals interactions, collectively reinforcing the binding stability of compound **6k** within the active site.

Gentamicin C1 exhibited a predominantly hydrogen-bond–driven interaction network with aromatic contributions limited to weak π–σ or π–alkyl contacts. In contrast, compound **6e** showed strong aromatic and hydrophobic π-interactions, arising mainly from its bulky naphthyl and phenethyl substituents. Compound **6k** had a balanced profile, combining hydrogen bonding, π-interactions, and halogen contacts, offering a more diversified interaction pattern than 6e including halogen bonding (GLU445) and additional hydrogen bonds contacts through its pyridyl nitrogen. This broader interaction network distinguishes compound **6k** from **6e**, resulting in improved relative binding affinity and enhanced adaptability within the binding pocket. Gentamicin, **6e**, and **6k** exhibit distinct binding modes arising from their diverse interaction profiles, as illustrated in Figure 6A, with a summary of the corresponding interactions provided in Table 2.

Molecular interaction profile of compounds with TrmD

Binding affinity outcomes against Pseudomonas aeruginosa TrmD indicated that compound **6k** (–7.5 kcal/mol) exhibited a stronger predicted binding affinity than compound **6e** (–7.1 kcal/mol) and 9D3 (–6.8 kcal/mol) (Table 3). Although compound **6k** showed a better predicted binding affinity toward TrmD than **6e** and 9D3, the *in vitro* activity favoured **6e**, suggesting that binding affinity alone does not fully account for antibacterial efficacy. This highlights the contribution of non-binding factors, such as physicochemical properties and bacterial cell barriers, in determining overall biological performance.

Compound 9D3 shares a scaffold similar to the evaluated compounds but features a predominant substitution on the thieno ring, consisting of a carboxamide linker connected to a methylphenyl ring bearing a diethylamino substituent. The interaction profile of 9D3 includes a hydrogen-bond interaction with LEU143. The phenyl ring forms a π–π T-shaped interaction with TYR120, while an amide–π stacking interaction is observed between SER93 and the thieno-pyrimidinone core. Additionally, PRO94, ILE138, and PRO149 participate in π–alkyl interactions, and GLY139 contributes a C–H bond interaction. An unfavourable acceptor–acceptor interaction is observed with TYR141 involving the backbone scaffold, whereas TYR120 also engages in alkyl interactions with the ethyl moiety of the diethylamine substituent. Furthermore, nearby binding-site

 doi:10.20944/preprints202603.1622.v1

residues SER137, TRP136, LEU92, GLY146, GLY118, GLY145, VAL142, ARG119, GLU121, and SER144 contribute stabilizing van der Waals interactions.

Although **6e** and **6k** share a similar core scaffold with 9D3, substitutions on both the thieno and pyrimidinone rings give rise to a slightly distinct interaction profile and binding orientation, as illustrated in Figures 4B.

Compound **6e** formed a hydrogen-bond interaction with TYR91 involving the sulfur atom of the thieno ring. Notably, its hydrophobic stacking interactions showed similarities to those observed for 9D3, engaging the same key residues TYR120 and SER93 in a comparable manner. Specifically, TYR120 exhibited a π–π T-shaped interaction with the naphthyl moiety, while SER93 participated in an amide–π stacking interaction with the phenyl ring. In addition, PRO94 displayed π–alkyl interactions with both the scaffold and the phenyl ring, whereas PRO149 engaged in π–alkyl interactions exclusively with the phenyl ring; both proline residues exhibited interaction patterns similar to those observed in 9D3. LEU143, which participates in a π–alkyl interaction in 6e, formed a hydrogen bond in the 9D3 complex. Furthermore, multiple van der Waals interactions were observed with surrounding binding-site residues, including ILE123, GLY122, GLN95, GLY118, ARG119, SER144, GLY145, VAL142, TYR141, GLY139, ILE138, SER137, TRP136, GLY146, and LEU92, collectively contributing to enhanced ligand stabilization within the active site

Compound **6k** exhibited a hydrogen-bond interaction pattern similar to that of **6e**, involving TYR91 through the thieno ring. In addition, an extra hydrogen-bond interaction was observed with SER137, mediated by the chloro substituent on the phenyl ring. A distinct π–σ interaction with GLY122, involving the thieno ring, was also identified. Furthermore, a triad of alkyl and π–alkyl interactions involving PRO94, ILE138, and PRO149 was observed; notably, this same set of residues displayed comparable interactions in the 9D3 complex. LEU143 engaged in both a π–alkyl interaction with the phenyl ring and a C–H bond interaction with the ethyl linker. Additionally, multiple surrounding binding-site residues, including LEU92, ILE123, GLU121, GLY146, GLY139, TYR141, VAL142, GLY145, ARG119, GLN95, TYR120, GLY118, and SER144, contributed stabilizing van der Waals interactions, collectively supporting the binding of compound **6k** within the active site.

For both **6e** and **6k**, TYR91 contributes to ligand stabilization through concurrent hydrogen-bonding and π–sulfur interactions with the thieno moiety. A summary of these interaction details is presented in Table 3.

Compounds 9D3, **6e** and **6k** share a common thieno-pyrimidinone scaffold and display overlapping binding modes within the same active-site pocket, engaging a conserved set of residues and adopting closely aligned binding orientations (Figure 6B). Across all three protein-ligand complexes, TYR120 and SER93 play central roles in aromatic stacking interactions, while PRO94, ILE138, and PRO149 consistently contribute π–alkyl or alkyl interactions, reflecting a shared hydrophobic interaction framework. LEU143 is involved in ligand stabilization in all cases, although the nature of the interaction varies (hydrogen bonding in 9D3 versus π–alkyl or C–H interactions in **6e** and **6k**). Overall, the similarities highlight a conserved recognition framework, with differences arising mainly from substituent-driven modulation of interaction types.

Figures 4 and 5 provide a comprehensive visualization of the distinct interaction profiles of compounds **6e** and **6k** within the active sites of *S. aureus* aminoglycoside phosphotransferase and *P. aeruginosa* TrmD, respectively. Figures 7 and 8 further depict the corresponding binding sites and pocket conformations of the evaluated compounds, offering deeper insight into their molecular recognition patterns and binding behavior

Determination of ADMET profile, Lipinski rule, and pharmacokinetics

ADMET profiling was performed to evaluate the pharmacokinetic behavior of the selected compounds. Absorption, distribution, metabolism, and excretion properties were predicted using the SwissADME platform (http://www.swissadme.ch/) [33], offering insights into their drug-likeness and key physicochemical features. Toxicological profile was assessed via the pkCSM webserver (https://biosig.lab.uq.edu.au/pkcsm/prediction) [34]. These computational assessments provided preliminary insights into the safety and pharmaceutical characteristics of the compounds.

 doi:10.20944/preprints202603.1622.v1

Table 4. Pharmacokinetic properties prediction with SWISS ADME.

Parameters	6e	6k
Molecular Weight (g/mol)	382.48	367.85
Log P o/w	5.19	3.98
No. of. H-bond Donors	0	0
No. of H-bond Acceptors	2	3
No.of rotatable bonds	4	4
Solubility	Poor	Moderate
TPSA(Å²)	63.13	76.02
GI absorption	High	High
BBB permeation	No	No
P-gp substrate	Yes	No
Drug likeness (Lipinski)	Yes; 1 violation: MLOGP>4.15	Yes
CYP450 isoforms inhibition	CYP1A2, CYP2C19, CYP2C9, CYP3A4	CYP1A2, CYP2C19, CYP2C9, CYP3A4
Bioavailability score	0.55	0.55

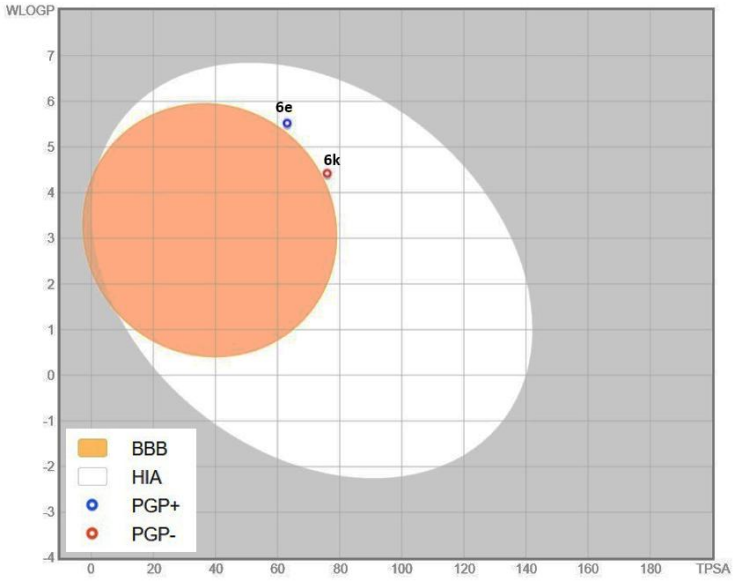

Figure 9. The Brain Or Intestinal Estimated Permeation (BOILED-Egg) method [35] illustrates the absorption, blood-brain barrier (BBB) permeation, and substrate selectivity for P-glycoprotein (PGP) of compounds **6e** and **6k**. Blue indicates substrate of P-glycoprotein (PGP), while red represents non-substrate of PGP.

 doi:10.20944/preprints202603.1622.v1

Table 5. Toxicological profile of compounds with pkCSM.

Parameters	6e	6k
AMES toxicity	No	Yes
hHERG I inhibition	No	No
hHERG II inhibition	Yes	Yes
Hepatotoxicity	Yes	Yes
Skin Sensitisation	No	No

In silico ADME assessment revealed that compounds **6e** and **6k** share largely overlapping pharmacokinetic characteristics. Both candidates are predicted to exhibit efficient high gastrointestinal (GI) absorption, absence of BBB permeation suggesting minimal CNS exposure and an identical bioavailability score (0.55). Compliance with Lipinski's criteria was observed for both molecules; however, compound **6e** had a violation due to elevated lipophilicity (MLOGP > 4.15). Structural differences between the two compounds are manifested in their polarity-related descriptors, with **6k** possessing an additional hydrogen bond acceptor and a correspondingly increased topological polar surface area (TPSA) (76.02 Å² vs. 63.13 Å²). These features translate into a more favorable solubility profile for 6k, which is predicted to have moderate aqueous solubility, whereas **6e** is associated with limited solubility. Predicted CYP450 inhibition is similar for **6e** and **6k** across the major isoforms (CYP1A2, CYP2C19, CYP2C9, and CYP3A4). A summary of these details is provided in Table 4 for reference.

The comparative analysis highlights **6k** as pharmacokinetically more balanced than **6e**. The lower molecular weight and reduced lipophilicity (LogP 3.98 vs. 5.19) of **6k** are advantageous, as excessive lipophilicity in **6e** may contribute to poor aqueous solubility, increased nonspecific binding, and higher metabolic liabilities. Compound **6k** combines higher polarity with good permeability, resulting in improved solubility and maintained higher GI absorption.

Notably, **6e** is predicted to be a P-gp substrate, which may limit its effective intracellular accumulation due to efflux mechanisms, whereas **6k** lacks this liability, potentially offering superior systemic exposure. Despite comparable CYP450 inhibition profiles, the metabolic liability of drug–drug interactions is greater for **6e** owing to its less favorable lipophilicity and solubility. Figure 9 presents these pharmacokinetic features using the BOILED-Egg model, highlighting GI absorption, BBB permeability, and P-gp interactions.

Overall, within the scope of the exploratory *in silico* ADME evaluation, compound 6k exhibits a more favorable drug-like profile, characterized by improved solubility, balanced lipophilicity, higher predicted GI absorption, and lower efflux-associated liabilities. Collectively, these attributes support the prioritization of **6k** as a promising lead for further optimization toward enhanced pharmaceutical performance and therapeutic potential.

Predicted safety endpoints suggest that both **6e** and **6k** are associated with hERG II inhibition and potential hepatotoxic effects, pointing to possible risks involving cardiac repolarization and liver function. Genotoxicity predictions distinguish the two compounds, as **6e** is non-mutagenic, whereas **6k** is predicted to be AMES-positive that raises concerns regarding potential mutagenicity (Table 5). Thus, although **6k** may present advantages in pharmacokinetic and drug-like properties, its predicted genotoxic risk introduces a key safety challenge that must be addressed during lead optimization with structural modifications to mitigate this liability. No significant risks of skin sensitization were observed with both the compounds. These findings highlight the importance of incorporating toxicity-mitigation strategies to improve overall safety.

Supplementary Materials: Copies of NMR spectra of new compounds are available in Supplementary Materials.

Author Contributions: Gagik Melikyan performed the conceptualization, methodology. Lusine Karapetyan: the experimental work and writing – review & editing. Gayane Tokmajyan analyzed spectral data. Ravikumar

 doi:10.20944/preprints202603.1622.v1

Kapavarapu: performed the molecular docking studies and writing the results. Mane Tadevosyan and Hovik Panosyan performed the antibacterial screening. Anahit Hovhannisyan perfomed the data curation and drafted the manuscript. Ashot Saghyan perfoemed the Supervision, and overall refined the manuscript. All authors have read and approved the final version of the manuscript.

Declaration of Competing Interest: The authors declare that they have no known competing financial interests or personal relationships that could have appeared to influence the work reported in this paper.

Funding: This work was supported by institutional research facilities. No additional grants to carry out or direct this particular research were obtained.

References

1. G. K. Mukusheva, N. N. Toigambekova, V. A. Savelyev, A. I. Khlebnikov, L. G. Burova, S. D. Afanaseva, O. A. Nurkenov, A. S. Kishkentayeva, A. S. Olzhabayeva, Yu. V. Gatilov, R.B. Seidakhmetova, A. N. Evstropov, E. E. Shults, Synthesis, Antibacterial Properties and Molecular Docking Studies of Nitrogen Substituted 9-(((4X-But-2-ynyloxy)methyl)-1,2,3-triazolyl)–Cinchona Alkaloid Conjugates, *Molecules*, 2025, *30*, 4352-4381.
2. Galina N. Lipunova,Emiliya V. Nosova andValery N. Charushin, Quinazolines [*a*]-Annelated by Five-Membered Heterocycles: Synthesis and Biological Activity, *Molecules*, **2025**, *30*, 3506-3551.
3. A.S. Karandeeva, N. A. Bogdanova, M. V. Kabanova, S. I. Filimonov, Zh. V. Chirkova, A. A. Romanycheva, V. A. Panova, A. A. Shetnev, N. A. Togyzbayeva, S. A. Kanzhar, N. O. Appazov, K. Yu. Suponitsky, Diastereoselective Synthesis and Biological Evaluation of Spiro[chromane-2,4′-pyrimidin]-2′(3′*H*)-ones as Novel Antimicrobial and Antioxidant Agents, *Molecules*, **2025**, *30*, 2954-2974.
4. S. Alghawi, N. Sivakumar, S.H. A. Hassan, R. J. Abdel-Jalil Synthesis, Characterization, and Bioactivity Inves tigation of Novel Benzimidazole Derivatives as Potential Antibacterial and Antifungal Agents, *Molecules*, 2026, 31, 844-870.
5. J.P. Dupin, R.J. Gryglewski, D. Gravier, G. Hou,F. Casadebaig, J. Swies, S. Chlopicki, Synthesis and Thrombolytic Activity of New Thienopyrimidinone Derivatives. *J. Physiol. Pharamacol.* 53 (2002) 625.
6. A.T. Mavrova, S. Dimov, D. Yancheva, M. Rangelov, D. Wesselinova, E. Naydenova, New C2- and N3-Modified Thieno[2,3-d]Pyrimidine Conjugates with Cytotoxicity in the Nanomolar Range. *Anticancer Agents Med. Chem.* **2022**, 22, 1201.
7. P. Lagardère, C. Fersing, N. Masurier, V. Lisowski, Thienopyrimidine: A Promising Scaffold to Access Anti-Infective Agents. *Pharmaceuticals (Basel).* **2021**, 15, 35.
8. S. Malla, A. Nyinawabera, R. Neupane, R. Pathak, D. Lee, M. Abou-Dahech, S. Kumari, S. Sinha, Y. Tang, A. Ray, C.R. Jr. Ashby, M.Q. Yang, R.J. Babu, A.K. Tiwari, Novel Thienopyrimidine-Hydrazinyl Compounds Induce DRP1-Mediated Non-Apoptotic Cell Death in Triple-Negative Breast Cancer Cells. *Cancers (Basel).* **2024**, 16, 2621.
9. R.V. Chambhare, B.G. Khadse, A.S. Bobde, R.H. Bahekar, Synthesis and Preliminary Evaluation of Some N-[5-(2-furanyl)-2-methyl-4-oxo-4H-thieno-[2,3-d]pyrimidin-3-yl]-carboxamide and 3-Substituted-5-(2-furanyl)-2-methyl-3*H*-thieno-[2,3-d]pyrimidin-4-ones as Antimicrobial Agents. *Eur. J. Med. Chem.*, **2003**, 38, 89.
10. B. Narasimhan, M. Kumari, N. Jain, A. Dhake, C. Sundaravelan, Correlation of antibacterial activity of some N-[5-(2-furanyl)-2-methyl-4-oxo-4H-thieno[2,3-d]pyrimidin-3-yl]-carboxamide and 3-substituted-5-(2-furanyl)-2-methyl-3H-thieno[2,3-d]pyrimidin-4-ones with topological indices using Hansch analysis. *Bioorg. Med. Chem. Lett.* **2006**, 16, 4951.
11. M. J. Hossain, H. M. M. Bhuiyan Synthesis and Antimicrobial Activity of Some New Thieno and Furopyrimidine Derivatives. *J. Sci. Res.* **2009**, 1, 317.
12. A.-R. El-Gazzar, H.A.R. Hussein, H.N. Hafez Synthesis and Biological Evaluation of thieno[2,3-d] pyrimidine derivatives for anti-inflammatory, analgesic and ulcerogenic activity. *Acta Pharm.* **2007**, 57, 395.

 doi:10.20944/preprints202603.1622.v1

13. H. B. Borate, R. A. Annadate, S. S. Vagh, M. M. Pisal, S. B. Deokate, M. A. Arkile, N. J. Jadhav, L. U. Nawale, D. Sarkar, Synthesis and evaluation of thieno[2,3-*d*]pyrimidin-4(3*H*)-ones as potential antitubercular agents. *Med. Chem. Commun.* 2015, 6, 2209.
14. E. I. Elmongy, Thieno[2,3-*d*]pyrimidine derivatives: Synthetic approaches and their FLT3 kinase inhibition, *J. Heterocycl. Chem.* **2020**, 57, 2067.
15. E. Z. Elrazaz, R. A. T. Serya, N. S. M. Ismail, D. A. Abou El Ella, K. A. M. Abouzid, Thieno[2,3-*d*] pyrimidine based derivatives as kinase inhibitors and anticancer agents. *Future J. Pharm. Sci.* **2015**, 1, 33.
16. E. A. Sobh, M. A. Dahab, E. B. Elkaeed, B. A. Alsfouk, I. M. Ibrahim, A. M. Metwaly, I. H. Eissa, New thieno[2,3-*d*]pyrimidine derivatives as $EGFR^{WT}$ and $EGFR^{T790M}$ inhibitors: Design, synthesis, antiproliferative activities, docking studies, ADMET, toxicity, MD simulation studies. *J. Heterocycl. Chem.* **2024**, 61, 285.
17. B. Liu, G. He, Discovery of Thieno[3-d]pyrimidine-Based Hydroxamic Acid Derivatives as Bromodomain-Containing Protein 4/Histone Deacetylase Dual Inhibitors Induce Autophagic Cell Death in Colorectal Carcinoma Cells. *J. Med. Chem.* **2020**, 63, 3678.
18. K. Bozorov, J.Y. Zhao, B. Elmuradov, A. Pataer, H. A. Aisa, Recent developments regarding the use of thieno[2,3-d]pyrimidin-4-one derivatives in medicinal chemistry, with a focus on their synthesis and anticancer properties. *Eur. J. Med. Chem.* **2015**, 102, 552.
19. E. M. H. Ali, M. S. Abdel-Maksoud, Ch.-H. Oh Thieno[2,3-d]pyrimidine as a promising scaffold in medicinal chemistry: Recent advances. *Bioorg. Med. Chem.* **2019**, 27, 1159.
20. A.Hovhannisyan, L. A. Aristakesyan, G. S. Melikyan, Facile synyhesis of 5(6)-phenyl substituted thieno[2,3-d] pyrimidin-4-ones. *Proceedings of the YSU. Chem. and Bio. Sci.* **2013**, 47, 8.
21. A.Hovhannisyan, L. Aristakesyan, G. Melikyan Facile approach to the synthesis of substituted thieno[2,3-d] pyrimidin-4-ones. *Hetereocycl. Commmun.* **2012**, 18, 253.
22. A. Hovhannisyan, T.H. Pham, D. Bouvier, A. Piroyan, L. Dufau, L. Qin, Y. Cheng, G. Melikyan, M. Reboud-Ravaux, M. Bouvier-Durand New C4- and C1-derivatives of furo[3,4-c]pyridine-3-ones and related compounds: Evidence for site-specific inhibition of the constitutive proteasome and its immunoisoform. *Bioorg. Med. Chem. Lett.* **2014**, 24,1571.
23. A.Hovhannisyan, L.H. Aristakesyan, G.S. Melikyan Synthesis of 5-(4-chloro)- and (4-methyl)phenyl- substituted thieno[2,3-d]pyrimidin-4-ones. *Chem. J. Armenia* **2014**, 67, 464.
24. S. O. Vardanyan, A. A. Aghekyan, A. S. Avagyan, A. B. Sargsyan, H. A. Panosyan, S. A. Harutyunyan, H. V. Gasparyan, Synthesis of New 5-(1,4-Benzodioxan-2-yl)thieno[2,3-*d*]pyrimidine Derivatives, *Russ. J. Org. Chem.* **2022**, 58, 977.
25. S. O. Vardanyan, A. S. Avagyan, A. B. Sargsyan, S. A. Harutyunyan, H. V. Gasparyan, A. A. Aghekyan, Synthesis of substituted thienopyrimidinones based on 2-amino-4-(1,4-benzodioxan-2-yl)thiophene-3-carboxylic Acid Ethyl Ester. *Russ. J. Org. Chem.* **2025**, 61, 447.
26. T. Shi, L. Kaneko, M. Sandino, R. Busse, M. Zhang, D. Mason, J. Machulis, A. J. Ambrose, D. D. Zhang, E. Chapman, One-Step Synthesis of Thieno[2,3-*d*]pyrimidin-4(3*H*)-ones via a Catalytic Four-Component Reaction of Ketones, Ethyl Cyanoacetate, S_8, and Formamide. *ACS Sustainable Chem. Eng.* **2019**, 7, 1524.
27. K. Gewald, E. Schinke, H. Böttcher, Heterocyclen aus CH-Aciden Nitrilen, VIII. 2-Amino-Thiophene Aus Methylenaktiven Nitrilen, Carbonylverbindungen und Schwefel. *Chem. Ber.* **1966**, 99, 94-100.
28. A. Avetisyan, A. Djandjapanyan, M. Dangyan Investigations in the field of unsaturated lactones xxxi. Some chemical conversions of 2-acetyl-2-buten-4-olines. *Arm. Chem. J.*, **1977**, 30, 841.
29. S. Dallakyan, A. J Olson, Small-molecule library screening by docking with PyRx, *Methods in molecular biology (Clifton, N.J.)* **2015**, 1263, 243-250.
30. S.J. Caldwell, Y. Huang, A.M. Berghuis, Antibiotic Binding Drives Catalytic Activation of Aminoglycoside Kinase APH (2)-Ia, *Structure.* **2016**, 24, 935.
31. W. Zhong, K. Pasunooti, S. Balamkundu, Y.H. Wong, Q. Nah, V. Gadi, S. Gnanakalai, Y.H. Chionh, M.E. McBee, P. Gopal, S.H. Lim, N. Olivier, E.T. Buurman, T. Dick, C.F. Liu, J. Lescar, P.C. Dedon, Thienopyrimidinone Derivatives That Inhibit Bacterial tRNA (Guanine37-N1)-Methyltransferase (TrmD) by Restructuring the Active Site with a Tyrosine-Flipping Mechanism, *J. Med. Chem.* **2019,** 62, 7788.

 doi:10.20944/preprints202603.1622.v1

32. E.F. Pettersen, T.D. Goddard, C.C. Huang, E.C. Meng, G.S. Couch, T.I. Croll, J.H. Morris, T.E. Ferrin, UCSF ChimeraX: Structure visualization for researchers, educators, and developers. *Protein Sci.* **2021**, 30, 70.
33. Daina, O. Michielin, V. Zoete, Swiss ADME: a free web tool to evaluate pharmacokinetics, druglikeness and medicinal chemistry friendliness of small molecules, *Scientific reports* **2017**, 7, 42717.
34. D. E. V. Pires, T. L. Blundell, D. B. Ascher, pkCSM: Predicting small-molecule pharmacokinetic properties using graph-based signatures, *J. Med. Chem.* **2015**, 58, 4066.
35. Daina, V. Zoete, A BOILED-Egg to Predict Gastrointestinal Absorption and Brain Penetration of Small Molecules. *ChemMedChem.* **2016**, 11, 1117.